Dynamic Diffusive Interfacial Transport (D-DIT): A Novel Quantitative Swelling Technique for Developing Binary Phase Diagrams of Aqueous Surfactant Systems

Parth U. Kelkar,[1] Kendra A. Erk,[1] and Seth Lindberg[2,*]

[1]*School of Materials Engineering, Purdue University, West Lafayette, IN, 47907, USA*

[2]*Corporate Engineering, The Procter & Gamble Company, West Chester, OH, 45069, USA*

[*] Author to whom correspondence should be addressed. Electronic mail: lindberg.se@pg.com

Current methods to develop surfactant phase diagrams are time-intensive and fail to capture the kinetics of phase evolution. Here, the design and performance of a quantitative swelling technique to study the dynamic phase behavior of surfactants is described. The instrument combines cross-polarized optical and short-wave infrared (SWIR) imaging to enable high-resolution, high-throughput, and in-situ identification of phases and water compositions. Data across the entire composition spectrum for dynamics and phase evolution of a binary aqueous non-ionic surfactant solution at two isotherms is presented. This instrument provides pathways to develop non-equilibrium phase diagrams of surfactant systems – critical to predicting outcomes of formulation and processing. It can be applied to study time-dependent material relationships across a diverse range of materials and processes including dissolution of surfactant droplets and drying of aqueous polymer films.

I. INTRODUCTION

Surfactants are amphiphilic molecules that reduce surface tension and spontaneously self-assemble above the critical micelle concentration (CMC)[1]. In binary aqueous solutions, surfactants form an array of concentration- and temperature-dependent aggregates spanning from low-viscosity micellar phases to pasty, high-viscosity liquid crystalline phases such as hexagonal, cubic, and lamellar[2]. The self-assembly and associated phase information – including the number, structure, and composition of phases is typically documented in phase diagrams which are used to create various commercial products like shampoos and conditioners[3,4].

The study of surfactant phases is growing in both significance and complexity. Phase science is an old field[5–7] and classically, temperature-composition phase diagrams have been determined by sealing a priori known compositions in glass vials and observing the resulting phases. Krafft's pioneering work on the behavior of soap solutions in different solvents and the temperature dependence of soap crystal solubility set the stage for McBain's work leading to the first published phase diagram for a surfactant system (sodium laurate (dodecanoate)-sodium chloride-water ternary system at 90 °C) in 1922[8]. The first phase diagram for a binary system (potassium oleate-water) was published by McBain and Elford in 1926[9]. Historically, phase diagrams are developed over decades of carefully executed experiments. For example, the phase diagrams of the binary decyl tetraethylene glycol ether ($C_{10}E_4$)-H_2O[10] and dioctadecyldimethylammonium chloride (DODMAC)-H_2O[11] systems have been through numerous revisions. A complete phase diagram for the industrial workhorse sodium lauryl ether sulfate (SLES)-H_2O system has yet to be determined[12].

Current experimental methods for developing surfactant phase diagrams suffer from at least one of the following limitations: (1) the need to test many samples, (2) a low signal-to-noise ratio or poor accuracy, (3) expensive set-up and complicated data analysis, and (4) unable to capture transient phase dynamics. Isoplethal methods, such as polarized optical microscopy[13–15], calorimetry[16], and small angle x-ray scattering[17], are widely used but require testing of several samples[18]. Isothermal techniques like deuterium-based nuclear magnetic resonance (D-NMR)[19–21] and swelling (or penetration) experiments[7,22–24] can examine an wide concentration range but struggle with quantification of phase parameters and high-viscosity liquid crystalline phases[21].

In 1987, Laughlin and Munyon devised the first in-situ quantitative swelling method termed Diffusive Interfacial Transport (DIT), which overcame many of the limitations of classical techniques[4]. Similar to penetration experiments, the entire composition range could be investigated and all phases along an isotherm were produced. Data for the entire phase diagram could be obtained by conducting studies at several temperatures. In the first iteration of this method ("DIT-NDX"), a Jamin-Lebedeff quantitative split-beam transmission interferometer was coupled to a polarized optical microscope to measure the refractive indices of surfactant phases and determine their compositions[4,7]. The DIT-NDX technique produced a great deal of useful information[11,21,25], but the analytical accuracy of concentrations estimated using this method was poor. For example, the acylmethylglucamine phase diagram had to be adjusted based on separate calorimetric experiments[7].

The second version ("DIT-NIR") developed in 2000 used near-infrared (IR) microspectroscopy to measure water compositions instead of interferometry-based refractive index quantification[25]. The Jamin-Lebedeff optics from the earlier DIT-NDX were retained for qualitative analysis of surfactant phase textures based on polarized optical microscopy and an FT-NIR spectrophotometer coupled to an IR microscope was used to record IR spectra. DIT-NIR had many advantages over DIT-NDX[26] but was expensive to set up[27] and had poor signal-to-noise ratio, necessitating up to 128 scans to be co-added[25]. Further, generating concentrations from IR absorption spectra is difficult and Jamin-Lebedeff interferometers are no longer commercially available[21], impeding widespread use of this technique. Despite these limitations, the DIT-NIR technique had significant potential and, with appropriate system improvements, could serve as an efficient approach for constructing binary phase diagrams.

This article describes a new instrument called the “Dynamic-DIT” (D-DIT) which couples short-wave infrared (SWIR) imaging and polarized optical imaging to simultaneously track the temporal evolution of water concentration and phase formation. The D-DIT builds upon previous iterations of the Diffusive Interfacial Transport (DIT) methodology[4,25] and generates previously inaccessible data about kinetic phase transitions and equilibria of binary aqueous surfactant systems. The capability of the instrument is demonstrated by tracking the phase evolution of a binary aqueous non-ionic surfactant solution in a confined rectangular geometry over seven days.

II. EXPERIMENTAL SECTION

A. Experimental Setup

A schematic of the D-DIT is shown in **FIG. 1**. Visible light and SWIR radiation is transmitted through the D-DIT sample capillary and imaged with cameras. SWIR radiation is unaffected by polarizers. This experimental setup represents a novel integration of commercial instrumentation: a SWIR camera, an optical camera, an infrared radiation source, and a cold optical light source.

The instrumentation is controlled through a custom Python code that can initiate simultaneous image acquisition through both cameras at intervals as small as six seconds. The frames per second (fps) captured by the camera depend on pixel resolution and should be optimized. Only radiation from the composite light source was allowed to pass through the capillaries and be captured by the cameras. In a Dynamic-DIT experiment, pure or concentrated surfactant at one end (right) was brought in contact with water at the other open end (left) in a long, thin rectangular capillary (1D diffusion) **(supplementary material)**[18]. After the capillary was filled with water, the exposed end was sealed, e.g., with high-vacuum silicone grease. Post-initiation, capillaries were allowed to equilibrate at room temperature (22 °C) or in a refrigerator (4 °C).

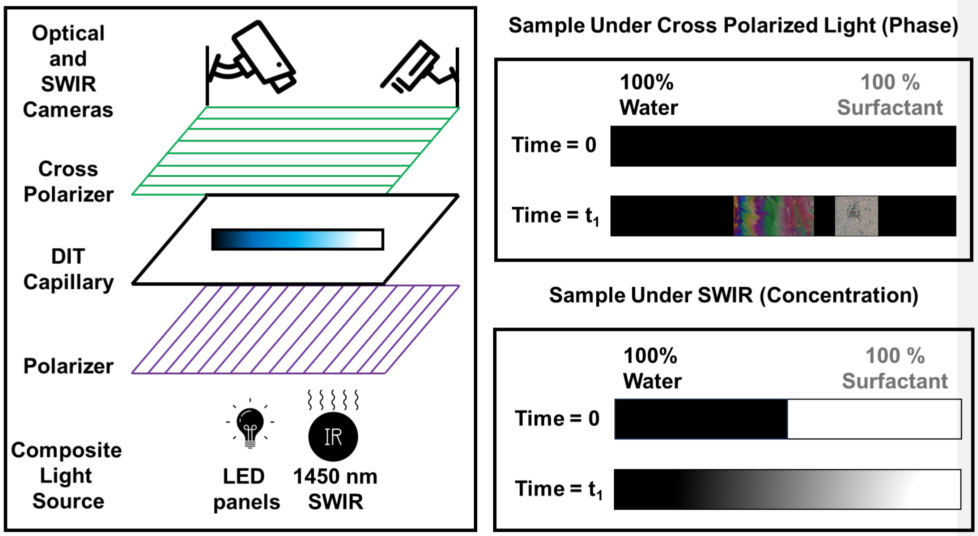

FIG. 1. Schematic of the novel D-DIT with three principal components – (1) composite light source (visible + SWIR), (2) Cross-polarizers and optical camera (phase structure), and (3) short-wave IR (SWIR) camera (water concentration). The instrument is pictured in the **supplementary material**.

1. Short Wave Infrared (SWIR) Camera

SWIR technology has been extensively used in defense applications[28] and was only declassified enough for public experimentation ~1995. More recently, it has been used for machine-vision inspection of silicon wafers and agricultural products[29,30]. An IR spectrum is produced by exciting various vibrational modes of a molecule with IR photons of varying wavelengths. The water molecule, which is a potent IR absorber, has three vibrational degrees of freedom: (1) symmetrical stretching, (2) asymmetric stretching, and (3) in-plane scissoring, with each mode corresponding to a unique wavenumber[31].

At a wavelength of approximately 1450 nm, liquid water exhibits a strong absorption band in the near-infrared region[32,33], causing objects with high moisture content to appear black in SWIR images. Surfactants and other molecules commonly encountered in surfactant systems, such as alcohols and carboxylic acids, do not absorb strongly in the same region of the IR spectrum as water[25]. The Goldeye G-033 TEC1 GigE SWIR camera has indium gallium arsenide (InGaAs) sensors and is sensitive to the SWIR spectrum between 900 and 1700 nanometers. It can capture up to 301 frames per second at 0.3-megapixel resolution and generate 14-bit images.

2. Optical Camera

The optical camera was used for imaging transmitted cross-polarized visible light. This setup utilized the Basler acA1920-50gc GigE color camera. It can capture 50 frames per second at a resolution of 2.3-megapixels and produce 12-bit images.

3. Composite Light source

The composite light source was a straightforward integration of commonly available cold LED panels and a 1450 nm SWIR backlight developed by EFFILUX. Both the sources were focused to get maximum radiation through the capillaries. Polarizing sheets were integrated above and below the capillaries to ensure cross-polarization of visible light.

4. DIT capillaries

Rectangular glass capillaries manufactured by Vitrocom with chamber dimensions 50 mm x 10 mm x 1 mm (length x width x thickness) were used in this study. The originally received capillaries were sealed at one end and displayed no strain birefringence. Capillaries were selected based on principles established by Laughlin et al.[4,25] – they were geometrically constrained to ensure that concentration gradients along the two short dimensions vanished, while the gradient along the longest dimension persisted. An additional consideration was IR transmission. The chamber had to be sufficiently thick for SWIR imaging with high contrast, but small enough to eliminate hydrodynamic effects.

B. Data Processing

Contrary to previous iterations of DIT, analyzing data from the D-DIT was straightforward and based on the Beer-Lambert Law[34] (**Equation (1)**). An empty capillary and a capillary filled with water were used as controls. Only water, and not the surfactant absorbed IR resulting in an intense black color that was tracked. A single sequence of images was sufficient and multiple scans were not necessary.

$$A = Log_{10}\frac{I_o}{I} = \varepsilon\, l\, c \quad (1)$$

I_o was the baseline intensity for the black capillary or capillary filled only with surfactant while I corresponded to the measured intensity post-initiation. The extinction coefficient ε for water was calculated from the loaded capillary at t = 0. The control capillary can also be used. Knowing the absorbance (A) and path length through the capillary (l = 1 mm), water concentration was determined and normalized to the length of the capillary (50 mm). Qualitative identification of surfactant phases from cross-polarized optical images was based on the classical work of Rosevear[15].

III. RESULTS AND DISCUSSION

To demonstrate the diverse capabilities of the D-DIT, simultaneous cross-polarized optical and SWIR imaging data is provided for the dynamic phase behavior of the non-ionic surfactant pentaethylene glycol monodecyl ether ($C_{10}E_5$) - linear formula $CH_3(CH_2)_9(OCH_2CH_2)_5OH$. An optically clear, liquid solution of $C_{10}E_5$ (BioXtra, ≥97.0% - Millipore Sigma) was used as received.

FIG. 2 shows high-resolution cross-polarized micrographs of capillaries seven days post-initiation of the DIT experiment.[15] Micellar and cubic phases appear dark under cross-polarizers[15]. At both temperatures, birefringent regions in **FIG. 2** (a – i) and (b – i) represented co-existing hexagonal and lamellar phases. The hexagonal phase could be identified by its characteristic fan-like structures **FIG. 2** (b – ii), while lamellar phases were determined by the presence of multilamellar vesicles (MLVs) (**FIG. 2** (a – ii) and (a - iii)).

Water concentration evolution data at two isotherms across the entire composition spectrum (0-100% water concentration) is presented in **FIG. 3** (a) and dynamic data over the initial 8 hours post-initiation at 22 °C is available **(multimedia view)**. As expected[7], the concentration gradient was initially steep (**FIG. 3** (a): t = 0 days) and gradually started to smoothen (**FIG. 3** (a) – t = 1 day) with countercurrent diffusion of solute and solvent. Seven days after initiation at 22 °C (**FIG. 3** (a) – t = 7 days), water diffused to the closed end of the capillary and resulted in two distinct phase regions (Micelles > Birefringent region (co-existing lamellar and hexagonal phases)) as seen in **FIG. 2** (b - i).

At 4 °C, five distinct phase bands – Micelles > Hexagonal > Cubic > Birefringent region (co-existing lamellar and hexagonal phases) > micelles (**FIG. 2** (b - i)) – were observed with decreasing water concentration. Water concentration at boundaries of phase bands is presented in **FIG. 3** (b). At this temperature, interdiffusion across the capillary was slower, and needle-like structures were observed at the liquid crystalline/ micellar interface (**FIG. 2** (b - iii)).

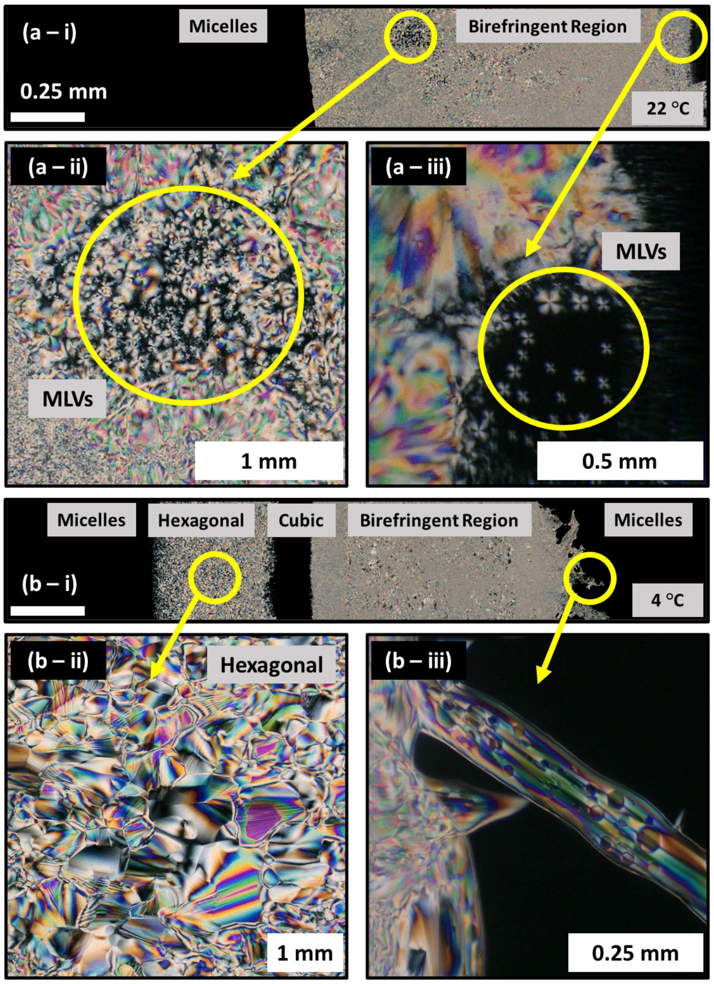

FIG. 2. $C_{10}E_5$ – water capillaries at t = 7 days at (a - i) 22 °C, and (b - i) 4 °C. Specific features of interest shown in (a – ii), (a – iii), (b – ii), and (b – iii). Scale bars in (a – i) and (b – i) indicate 2.5 mm. High-resolution cross-polarized micrographs captured using a Keyence VHX-F series microscope equipped with a Dual-Objective VH-ZST Zoom Lens (magnification range

20x to 2000x) with polarizers). Full images from the D-DIT are presented in the **supplementary material.**

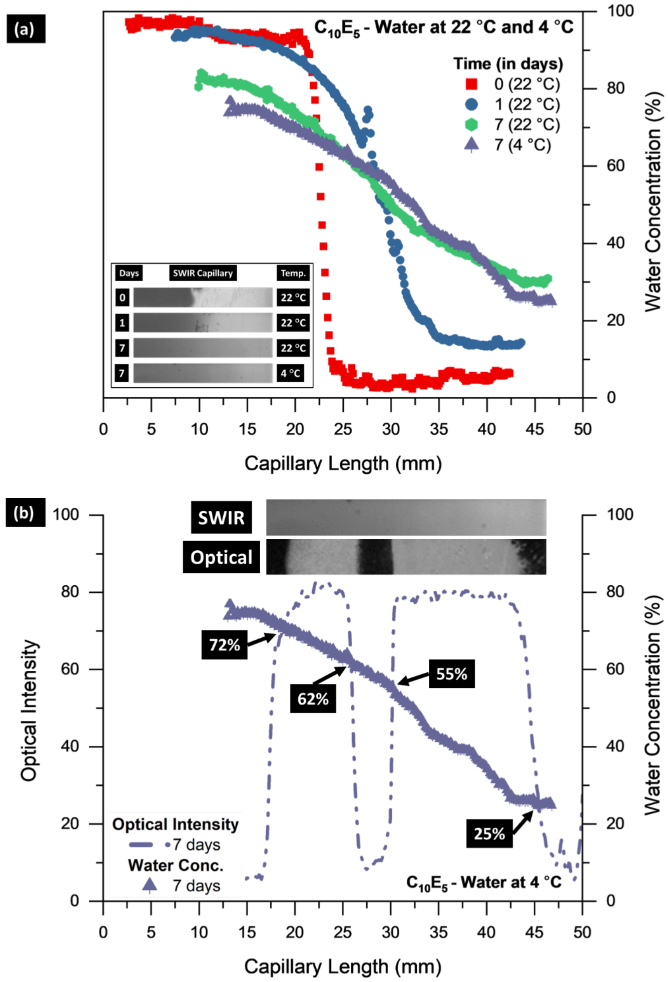

FIG. 3. (a) Evolution of water concentration profiles. (Inset) SWIR images of line scans across the capillary **(multimedia view)**. (b) Optical intensity and water concentration profile across the length of the capillary at 4 °C. (Inset) corresponding line scans from SWIR and optical images.

Width of the phase bands can be determined from points of intersection of intensity and concentration profiles (intersections indicated by arrows). A complete set of profiles is shown in the **supplementary material.**

Water concentrations at selected points of interest and comparisons to the equilibrium phase diagram developed by Nibu and Inoue[16] are presented in **FIG. 4** (b). There was good correlation between water content and predicted phases at 22 °C, with the exception of an optically isotropic micellar phase formed between the hexagonal and lamellar phases[16]. In this study, no such phase was found. The absence of this micellar phase and the presence of a coexisting birefringent region were attributed to two key factors: (1) the high degree of packing of lamellar and hexagonal phases leading to slower water diffusion; and (2) extremely high viscosity of the hexagonal phase restricting flow and movement in the capillary. The complexity is further increased by the fact that the 22 °C isotherm is close to the upper limit of the hexagonal phase boundary.

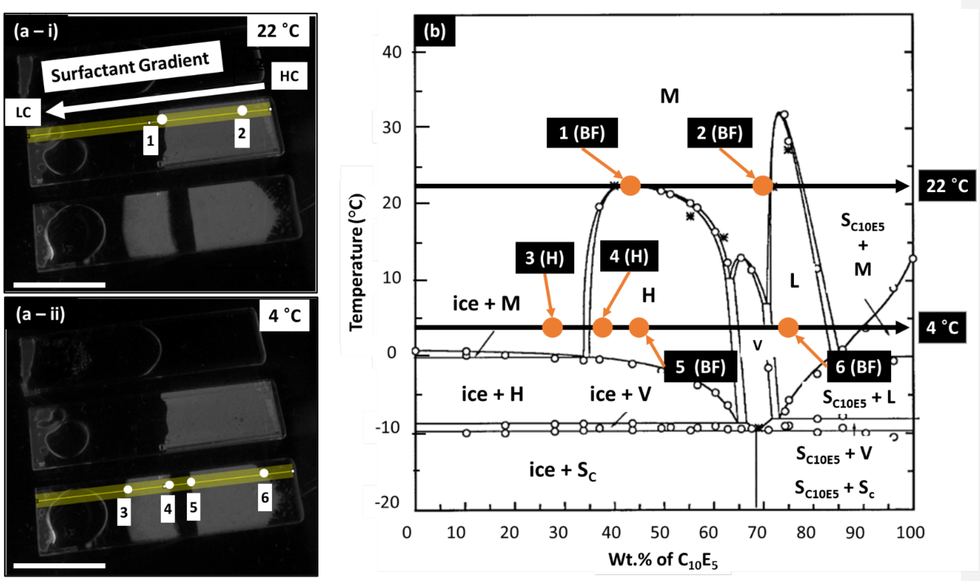

FIG. 4. (a-i) and (a-ii) Cross-polarized optical images at 22 °C and 4 °C after 7 days with water gradient from left to right and corresponding $C_{10}E_5$ gradient from right to left (HC - high concentration and LC - low concentration). Points of interest are marked 1-6. Scale bars (lower left) indicate 20 mm. (b) Comparison between selected points of interest (1-6) from D-DIT capillaries and equilibrium $C_{10}E_5$ – water phase diagram adapted from Nibu and Inoue[16]. Legend: M – Micelles, H – Hexagonal phase, V – Cubic phase, L – Lamellar phase, S_c – solid phase hydrated compound, S_{C10E5} - solid of pure $C_{10}E_5$, and BF – birefringent region (with coexisting Hexagonal (H) and Lamellar (L) phases). Phases identified are written in circular brackets (E.g., 1(BF) indicates point 1 from (a-i) and its phase BF.)

All expected phases were observed at 4 °C. However, the water concentration and the resulting phases, along with the position of the phase bands did not align with those predicted by the equilibrium phase diagram[16]. This was extremely interesting and alluded to the interplay between the kinetics of mass transport across interfaces to reach equilibrium in a confined environment and the dynamic nature of the measurements. Small temperature changes developed while imaging the capillary at room temperature (22 °C) could have also induced another non-equilibrium effect - efforts were made to minimize time spent outside the temperature conditioning environment. Over time, it is expected that the phase bands will asymmetrically widen[4] and the capillary will equilibrate to a uniform concentration.

IV. DISCUSSION

The Dynamic-DIT can develop non-equilibrium phase diagrams of surfactant systems, which are fundamentally distinct from equilibrium temperature-concentration diagrams. By considering the time required for a system to reach equilibrium, non-equilibrium phase diagrams can be used to predict the outcomes of various processes like dilution, mixing, and temperature changes. Additionally, the dynamics of phase transitions in geometrically constrained environments can be utilized in products and flow processes to kinetically trap the surfactant in desired non-equilibrium states[35].

It can also be used to quantify the dissolution and drying of surfactant or polymer solutions. Aqueous surfactant solutions, especially the low-viscosity micellar phases, are commonly used in personal care products like shampoos and detergents[2]. To lower a product's carbon and water footprint, global consumer product companies are striving to formulate, and ship concentrated products with high-viscosity liquid crystalline or gel phases[36]. However, such concentrated materials can reduce mixing and pumping efficiency during formulation and slow production[37,38]. During the processing of surfactant solutions, knowledge of the temperature-concentration phase diagram (hydration) and transformation kinetics from one phase to another (dissolution) is of paramount importance[39,40]. Other applications such as paper coatings[41,42], adhesives[43,44], pharmaceutical packaging[45], and printed circuit boards[46] make extensive use of water-based polymer films. Drying (inverse hydration) time is an essential processing and performance criterion for these films[47,48]. Additional studies are in progress.

This technique can be extended to multicomponent mixtures by running full 900 nm - 1700 nm absorption spectrums for each component using broadband SWIR excitation light sources and selective bandpass filters in front of the cameras. Certain components could also be tagged with dyes and markers sensitive to specific wavelengths. However, diffusion of more than two components can get extremely complicated since the third (or higher) component may diffuse separately from its starting location (tie-line crossing is common in ternary systems and tie-triangles must be constructed[21,49,50]), and must be carefully considered. The capabilities of the D-DIT can be enhanced by the addition of an environmental chamber to enable in-situ temperature ramps. As some SWIR signals are temperature dependent, proper calibrations must be performed at each temperature of interest.

V. SUMMARY

The Dynamic-DIT (D-DIT) enables the simultaneous in-situ measurement of water concentration and surfactant phase evolution. The system benefits from the coupling of commercially available instruments to perform a diverse array of experiments on aqueous solutions. The aqueous surfactant system characterized in this study is intended to demonstrate the capability of the Dynamic-DIT to characterize dynamic phase transitions and develop non-equilibrium phase diagrams. Experiments performed thus far represent only a small subset of the instrument's full capabilities as the SWIR camera can also be used for dissolution and drying studies. With further system improvements, the effects of various confining geometries and in-situ temperature variations on the dynamic behavior of surfactant phases can be investigated.

SUPPLEMENTARY MATERIAL

See supplementary material for optical and SWIR images from D-DIT, and complete coupled optical intensity and water concentration profiles. Multimedia files include D-DIT data over the initial eight hours at 22 °C.

ACKNOWLEDGEMENTS

P.U.K. and K.A.E. acknowledge support from the National Science Foundation (NSF) through GOALI Grant No. CBET-2112956. Fruitful discussions with a number of P&G scientists are also acknowledged, including Dr. Marco Caggioni, Dr. Alex Pinyayev and Dr. Paul Thomas.

CONFLICTS OF INTEREST

There are no conflicts of interest to declare.

AUTHOR CONTRIBUTIONS

P.U.K.: data curation, formal analysis, investigation, methodology, visualization, writing - original draft; K.A.E.: conceptualization, data curation, funding acquisition, project administration, visualization, supervision, writing - original draft, writing – review & editing; S.L.: conceptualization, data curation, methodology, funding acquisition, resources, supervision, writing – review & editing.

DATA AVAILABILITY

The data that support the findings of this study are available from the corresponding author upon reasonable request.

REFERENCES

[1] S. Ghosh, A. Ray, and N. Pramanik, "Self-assembly of surfactants: An overview on general aspects of amphiphiles," Biophys Chem **265**, 106429 (2020).

[2] J. Scamehorn, D. Sabatini, and J. Harwell, in *Encyclopedia of Supramolecular Chemistry* , 1st ed. (CRC Press, Boca Raton, 2004).

[3] P. Spicer, "Cubosome ProcessingIndustrial Nanoparticle Technology Development," Chemical Engineering Research and Design **83**(11), 1283–1286 (2005).

[4] R.G. Laughlin, and R.L. Munyon, "Diffusive interfacial transport: a new approach to phase studies," J Phys Chem **91**(12), 3299–3305 (1987).

[5] J.W. Gibbs, *The Collected Works of J. Willard Gibbs* (Longmans, Green and Co., New York , 1928).

[6] J.W. Cahn, "'Die heterogenen gleichgewichte (The Heterogeneous Equilibria)' a century later," Journal of Phase Equilibria **21**(4), 325–335 (2000).

[7] R.G. Laughlin, *The Aqueous Phase Behavior of Surfactants* (Academic Press, 1994).

[8] J.W. McBain, and A.J. Burnett, "CLVII.—The effect of an electrolyte on solutions of pure soap. Phase-rule equilibria in the system sodium laurate–sodium chloride–water," J. Chem. Soc., Trans. **121**(0), 1320–1333 (1922).

[9] J.W. McBain, and W.J. Elford, "LV.—The equilibria underlying the soap-boiling processes. The system potassium oleate–potassium chloride–water," J. Chem. Soc. **129**(0), 421–438 (1926).

[10] Y. Nibu, and T. Inoue, "Solid-Liquid Phase Behavior of Binary Mixture of Tetraethylene Glycol Decyl Ether and Water," J Colloid Interface Sci **205**(2), 231–240 (1998).

[11] R.G. Laughlin, R.L. Munyon, Y.C. Fu, and A.J. Fehl, "Physical science of the dioctadecyldimethylammonium chloride-water system. 1. Equilibrium phase behavior," J Phys Chem **94**(6), 2546–2552 (1990).

[12] R. L. Hendrikse, A. E. Bayly, and P. K. Jimack, "Studying the Structure of Sodium Lauryl Ether Sulfate Solutions Using Dissipative Particle Dynamics," J Phys Chem B **126**(40), 8058–8071 (2022).

[13] F. Reinitzer, "Beiträge zur Kenntniss des Cholesterins," Monatshefte Für Chemie - Chemical Monthly **9**(1), 421–441 (1888).

[14] P.G. Hartley, and H.-H. Shen, in *Self-Assembled Supramolecular Architectures* (John Wiley & Sons, Inc., Hoboken, NJ, USA, 2012), pp. 97–127.

[15] F.B. Rosevear, "The microscopy of the liquid crystalline neat and middle phases of soaps and synthetic detergents," J Am Oil Chem Soc **31**(12), 628–639 (1954).

[16] Y. Nibu, and T. Inoue, "Phase Behavior of Aqueous Mixtures of Some Polyethylene Glycol Decyl Ethers Revealed by DSC and FT-IR Measurements," J Colloid Interface Sci **205**(2), 305–315 (1998).

[17] E.A. Caicedo-Casso, J.E. Bice, L.R. Nielsen, J.L. Sargent, S. Lindberg, and K.A. Erk, "Rheo-physical characterization of microstructure and flow behavior of concentrated surfactant solutions," Rheol Acta **58**(8), 467–482 (2019).

[18] R.G. Laughlin, "The role of swelling methods in surfactant phase science: past, present, and future," Adv Colloid Interface Sci **41**, 57–79 (1992).

[19] P. Alexandridis, U. Olsson, and B. Lindman, "A Record Nine Different Phases (Four Cubic, Two Hexagonal, and One Lamellar Lyotropic Liquid Crystalline and Two Micellar Solutions) in

a Ternary Isothermal System of an Amphiphilic Block Copolymer and Selective Solvents (Water and Oil)," Langmuir **14**(10), 2627–2638 (1998).

[20] B. Lindman, U. Olsson, and O. Soderman, in *Dynamics of Solutions and Fluid Mixtures by NMR*, edited by J.-J. Delpuech (Wiley,1995).

[21] R.G. Laughlin, "Methodologies for phase studies of amphiphilic compounds: recent developments," Curr Opin Colloid Interface Sci **6**(4), 405–411 (2001).

[22] A.S. Poulos, C.S. Jones, and J.T. Cabral, "Dissolution of anionic surfactant mesophases," Soft Matter **13**(31), 5332–5340 (2017).

[23] R.I. Castaldo, R. Pasquino, M.M. Villone, S. Caserta, C. Gu, N. Grizzuti, S. Guido, P.L. Maffettone, and V. Guida, "Dissolution of concentrated surfactant solutions: from microscopy imaging to rheological measurements through numerical simulations," Soft Matter **15**(41), 8352–8360 (2019).

[24] I.D. Leigh, M.P. McDonald, R.M. Wood, G.J.T. Tiddy, and M.A. Trevethan, "Structure of liquid-crystalline phases formed by sodium dodecyl sulphate and water as determined by optical microscopy, X-ray diffraction and nuclear magnetic resonance spectroscopy," Journal of the Chemical Society, Faraday Transactions 1: Physical Chemistry in Condensed Phases **77**(12), 2867 (1981).

[25] R.G. Laughlin, M.L. Lynch, C. Marcott, R.L. Munyon, A.M. Marrer, and K.A. Kochvar, "Phase Studies by Diffusive Interfacial Transport Using Near-Infrared Analysis for Water (DIT-NIR)," J Phys Chem B **104**(31), 7354–7362 (2000).

[26] C. Marcott, R.G. Laughlin, A.J. Sommer, and J.E. Katon, in (1990), pp. 71–86.

[27] N.A. Blumenschein, D. Han, M. Caggioni, and A.J. Steckl, "Magnetic Particles as Liquid Carriers in the Microfluidic Lab-in-Tube Approach To Detect Phase Change," ACS Appl Mater Interfaces **6**(11), 8066–8072 (2014).

[28] K. Chrzanowski, "Review of night vision technology," Opto-Electronics Review **21**(2), (2013).

[29] A. Jenal, G. Bareth, A. Bolten, C. Kneer, I. Weber, and J. Bongartz, "Development of a VNIR/SWIR Multispectral Imaging System for Vegetation Monitoring with Unmanned Aerial Vehicles," Sensors **19**(24), 5507 (2019).

[30] A. Jenal, U. Lussem, A. Bolten, M.L. Gnyp, J. Schellberg, J. Jasper, J. Bongartz, and G. Bareth, "Investigating the Potential of a Newly Developed UAV-based VNIR/SWIR Imaging System for Forage Mass Monitoring," PFG – Journal of Photogrammetry, Remote Sensing and Geoinformation Science **88**(6), 493–507 (2020).

[31] U. Ritgen, in *Analytical Chemistry I* (Springer Berlin Heidelberg, Berlin, Heidelberg, 2023), pp. 219–238.

[32] R.A. Viscarra Rossel, and A.B. McBratney, "Laboratory evaluation of a proximal sensing technique for simultaneous measurement of soil clay and water content," Geoderma **85**(1), 19–39 (1998).

[33] R.H. Wilson, K.P. Nadeau, F.B. Jaworski, B.J. Tromberg, and A.J. Durkin, "Review of short-wave infrared spectroscopy and imaging methods for biological tissue characterization," J Biomed Opt **20**(3), 030901 (2015).

[34] J. Clark, and G. Gunawardena, "The Beer-Lambert Law," LibreTexts Chemistry, (CC BY-NC 4.0 license, Accessed 8/29/2023).

[35] S.S. Chittari, A.C. Obermeyer, and A.S. Knight, "Investigating Fundamental Principles of Nonequilibrium Assembly Using Temperature-Sensitive Copolymers," J Am Chem Soc **145**(11), 6554–6561 (2023).

[36] J.B. Aguiar, A.M. Martins, C. Almeida, H.M. Ribeiro, and J. Marto, "Water sustainability: A waterless life cycle for cosmetic products," Sustain Prod Consum **32**, 35–51 (2022).

[37] B. Kim, M.H. Siddique, A. Samad, G. Hu, and D.-E. Lee, "Optimization of Centrifugal Pump Impeller for Pumping Viscous Fluids Using Direct Design Optimization Technique," Machines **10**(9), 774 (2022).

[38] W. Monte Verde, E. Kindermann, J.L. Biazussi, V. Estevam, B.P. Foresti, and A.C. Bannwart, "Experimental Investigation of the Effects of Fluid Viscosity on Electrical Submersible Pumps Performance," SPE Production & Operations **38**(01), 1–19 (2023).

[39] H. Wang, S. Khodaparast, J. Carroll, C. Kelly, E.S.J. Robles, and J.T. Cabral, "A microfluidic-multiwell platform for rapid phase mapping of surfactant solutions," Review of Scientific Instruments **91**(4), (2020).

[40] J.C.R. Thacker, D.J. Bray, P.B. Warren, and R.L. Anderson, "Can Machine Learning Predict the Phase Behavior of Surfactants?," J Phys Chem B **127**(16), 3711–3727 (2023).

[41] N.M. Ryan, G.M. Mcnally, and J. Welsh, "The Use of Aqueous-based Emulsion Polymers as Moisture Barrier Coatings for Carton Boards," Developments in Chemical Engineering and Mineral Processing **12**(1–2), 141–148 (2004).

[42] J. Vyorykka, K. Zuercher, and D. Malotky, Paper Conference and Trade Show 2011(PaperCon2011). 2, 1051 (2011).

[43] D. Arunbabu, H. Shahsavan, W. Zhang, and B. Zhao, "Poly(AAc- *co* -MBA) Hydrogel Films: Adhesive and Mechanical Properties in Aqueous Medium," J Phys Chem B **117**(1), 441–449 (2013).

[44] M. Gerst, G. Auchter, G. Fonseca, and C.P. Beyers, United States Patent. US9.273,236 B2 (2016).

[45] S. Karki, H. Kim, S.-J. Na, D. Shin, K. Jo, and J. Lee, "Thin films as an emerging platform for drug delivery," Asian J Pharm Sci **11**(5), 559–574 (2016).

[46] C. Weiss, and H. Muenstedt, “Surface modification of polyether ether ketone (peek) films for flexible printed circuit boards,” J Adhes **78**(5), 443–445 (2002).

[47] N. Allanic, P. Salagnac, and P. Glouannec, “Study of the Drying Behavior of Poly(vinyl alcohol) Aqueous Solution,” Macromol Symp **222**(1), 253–258 (2005).

[48] I. Ludwig, W. Schabel, P. Ferlin, J.-C. Castaing, and M. Kind, “Drying, film formation and open time of aqueous polymer dispersions,” Eur Phys J Spec Top **166**(1), 39–43 (2009).

[49] N. Bezlyepkina, R.S. Gracià, P. Shchelokovskyy, R. Lipowsky, and R. Dimova, “Phase Diagram and Tie-Line Determination for the Ternary Mixture DOPC/eSM/Cholesterol,” Biophys J **104**(7), 1456–1464 (2013).

[50] S.P.A. Gill, in *Thermodynamics, Kinetics and Microstructure Modelling* (IOP Publishing, 2022), pp. 4–1 to 4–11.

Deleted: open time of aqueous polymer dispersions,” Eur Phys J Spec Top **166**(1), 39–43 (2009).¶
¶
¶ ... [1]

Formatted: Font: 12 pt

Formatted: Left

Page 17: [1] Deleted **Parth Uday Kelkar** **1/24/24 8:57:00 PM**